Borane Cluster Photochemistry. 3. The Photochemistry and Organometallic Rearrangement Chemistry of σ-Metalated Small Borane Cluster Compounds[1]

Bruce H. Goodreau,[†] Lianna R. Orlando,[‡] and James T. Spencer*

Contribution from the Department of Chemistry and the W. M. Keck Center for Molecular Electronics, Center for Science and Technology, Syracuse University, Syracuse, New York 13244-4100

Received June 6, 1995[⊗]

Abstract: The photochemistry of σ-metalated pentaborane(9) complexes [2-(Fe(η^5-C_5H_5)$(CO)_2$)B_5H_8] (**1**) and [2,4-(Fe(η^5-C_5H_5)$(CO)_2$)$_2B_5H_7$] (**2**) is described. These compounds readily undergo a clean photoinduced decarbonylation reaction to lose a carbon monoxide ligand upon irradiation to generate an unsaturated, 16-electron iron intermediate. The isolated products arise from the insertion of the reactive 16-electron iron center into the basal plane of the borane cluster. Thus, the conversion of the square-pyramidal B_5 cluster complexes, **1** and **2**, into the pentagonal-pyramidal FeB_5 vertex complexes, 2-(η^5-C_5H_5)-2-(CO)-2-FeB_5H_8 (**3**) and 4-(Fe(η^5-C_5H_5)$(CO)_2$)-2-(η^5-C_5H_5)-2-(CO)-2-FeB_5H_7 (**4**), respectively, was observed. The complete characterization of the products by ^{1}H, ^{11}B NMR (including both 1D and 2D ^{11}B−^{11}B {^{1}H} COSY data), infrared, and mass spectral analyses are reported. The X-ray crystal structure of **3** is also reported. Upon extended UV irradiation of either complex **2** or **4**, the only products observed were the dimeric [Fe(η^5-C_5H_5)$(CO)_2]_2$ complex and complex **3**, which apparently arise from the light-induced fission of a terminal σ iron−cage bond. The formation of the dimeric [Fe(η^5-C_5H_5)$(CO)_2]_2$ complex in this photolysis was expected through a radical coupling process of the initially photogenerated [Fe(η^5-C_5H_5)$(CO)_2$]$^\bullet$ species. The other anticipated coupling product, [(Fe(η^5-C_5H_5)(CO))$B_5H_7]_2$, was not found, but rather the formation of complex **3** was observed, which presumably formed through the extraction a hydrogen atom by the intermediate radical [2-(Fe(η^5-C_5H_5)(CO))B_5H_7]$^\bullet$ complex. A unique rearrangement of complex **4** to a new isomer, [3-(Fe(η^5-C_5H_5)$(CO)_2$)-2-(η^5-C_5H_5)-2-(CO)-2-FeB_5H_7] (**5**) is also reported. Crystallographic data for **3**: space group *Pnma* (No. 62, orthorhombic), a = 14.889(1) Å, b = 9.4560(9) Å, c = 7.2838(9) Å, V = 1025.5(3) Å^3, Z = 4 molecules/cell, R_w = 0.037 for 959 independent reflections.

Introduction

Photochemical transformations are widely employed in both organic and organometallic chemistry and have been extensively used as synthetic strategies for the formation of a variety of new compounds.[2−4] Photochemical techniques have proven to be powerful synthetic tools, often furnishing facile pathways to species which are not preparable in other ways. In addition, photochemical pathways frequently provide extremely high selectivity for single reaction products. In contrast with thermally induced reactions, photochemical processes typically possess very high activation selectivities, may be initiated at very low temperatures in all three phases, and allow access to products not readily available to thermally induced reactions.[2]

Organic and organometallic photochemical reactions have recently been intensely investigated and a great deal is now known about the reaction profiles and mechanisms for many of these systems.[2−4] In organometallic systems, for example, the irradiation of transition metal complexes has been found to typically result in ligand dissociation, reductive elimination, or homolytic bond cleavage reactions. While organic and organometallic photochemistry has yielded a rich array of interesting and important new compounds, the potentially fertile field of the photochemistry of main group clusters, especially the boranes, has received only very limited attention.[5−8] In consideration of the enormous contribution photochemical studies have made to synthetic and mechanistic organic and organometallic chemistry, we have begun investigations into the photochemistry of cluster systems to more fully understand the potential applications of this powerful technique to clusters. In this paper, the photochemical transformations of Fe(η^5-C_5H_5)-$(CO)_2$ substituted pentaborane clusters is explored for the first time.

Detailed photochemical investigations of the [Fe(η^5-C_5H_5)-$(CO)_2$R] organometallic compounds have been reported in the literature.[9−11] The lowest excited state for many organometallic complexes, including the [Fe(η^5-C_5H_5)$(CO)_2$R] complexes,

[†] Current address: Henkel Corporation, Parker Amchem, 32100 Stevenson Highway, Madison Heights, Michigan 48071.

[‡] National Science Foundation Research Experiences for Undergraduates Participant 1990−1992.

[⊗] Abstract published in *Advance ACS Abstracts*, November 1, 1995.

(1) Part 2: Davis, C. M.; Spencer, J. T. *Inorg. Chim. Acta* **1993**, *212*, 317.

(2) (a) Turro, N. J. *Modern Molecular Photochemistry*; Benjamin/Cummings: Menlo Park, 1978. (b) Ferraudi, G. *Elements of Inorganic Photochemistry*; Wiley-Interscience: New York, 1988.

(3) Wrighton, M. S., Ed. Inorganic and Organometallic Photochemistry. *Adv. Chem. Ser.* **1978**, *168*.

(4) Geoffroy, G. L.; Wrighton, M. S. *Organometallic Photochemistry*; Academic Press: New York, 1979.

(5) (a) Grebenik, P. D.; Green, M. L. H.; Kelland, M. A.; Leach, J. B.; Mountford, P. *J. Chem. Soc., Chem. Commun.* **1989**, 1397. (b) Greenwood, N. N.; Greatrex, R. *Pure Appl. Chem.* **1987**, *59*, 857. (c) Astheimer, R. J.; Sneddon, L. G. *Inorg. Chem.* **1984**, *23*, 3207. (d) Fehlner, T. P. *J. Am. Chem. Soc.* **1978**, *100*, 3250. (e) Zweifel, G.; Clark, G. M.; Hancock, K. G. *J. Am. Chem. Soc.* **1971**, *93*, 1308. (f) Spencer, J. T.; Pourian, M. R.; Butcher, R. J.; Sinn, E.; Grimes, R. N. *Organometallics* **1987**, 6, 335. (g) Plotkin, J. S.; Sneddon, L. G. *J. Chem. Soc., Chem. Commun.* **1976**, 95.

(6) Fehlner, T. P. *J. Am. Chem. Soc.* **1977**, *99*, 8355.

(7) Sneddon, L. G.; Beer, D. C.; Grimes, R. N. *J. Am. Chem. Soc.* **1973**, *95*, 6623.

(8) Schultz, R. V.; Sato, F.; Todd, L. J. *J. Organomet. Chem.* **1977**, *125*, 115.

(9) Blaha, J. P.; Wrighton, M. S. *J. Am. Chem.* Soc. **1985**, *107*, 2694.

(10) Kazlauskas, R. J.; Wrighton, M. S. *Organometallics* **1982**, *1*, 602.

0002-7863/95/1517-11754$09.00/0

Scheme 1. Photochemistry of $[Fe(\eta^5\text{-}C_5H_5)(CO)_2(\mu\text{-}4,5\text{-}C_2B_4H_7)]$[7,8]

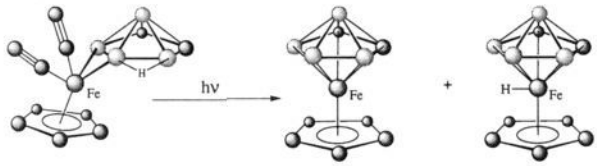

typically involves a M−L antibonding orbital leading dominantly to ligand dissociative processes as the primary photochemical step. For example, the irradiation of $[Fe(\eta^5\text{-}C_5H_5)(CO)_2\text{-}CH_3]$ in the presence of a suitable ligand, such as a phosphine, yielded exclusively the product resulting from CO ligand dissociation and coordination of the new ligand. The key intermediate in this process was believed to be the relatively long-lived, coordinatively unsaturated $[Fe(\eta^5\text{-}C_5H_5)(CO)CH_3]$ complex. Upon irradiation of the ethyl-substituted analogue, $[Fe(\eta^5\text{-}C_5H_5)(CO)_2(C_2H_5)]$, CO ligand dissociation was again observed first, followed by the rapid transfer of a β-hydride from the alkyl group to the metal center.[7] This β-hydride transfer was followed by olefin dissociation and ligand coordination, either of the initially photoejected CO or by recoordination of the olefin, to yield the observed products. Products which would arise from an intermediate involving either homolytic metal−L bond cleavage or alkyl migration reactions were not observed. Finally, in the case of the benzyl-substituted analogue, $[Fe(\eta^5\text{-}C_5H_5)(CO)_2(CH_2C_6H_5)]$, products from both CO dissociative and homolytic bond fission pathways were observed.[9] In this system, however, the CO dissociative process was found to occur with a much greater quantum efficiency than the homolytic M−R bond cleavage process.

Relatively little has been reported on the photochemistry of the metallaboranes. The photochemical reactions of several iron metallaboranes have, however, been previously reported.[6−8] In one report, it was observed that the irradiation of $[(Fe(\eta^5\text{-}C_5H_5)\text{-}(CO)_2B_{10}H_{13}]$ in ether yielded $[Fe(\eta^5\text{-}C_5H_5)B_{10}H_{10}C(L)]$ (where L = OEt_2 or THF) in 1 to 3% yield.[8] This unexpected observed product apparently resulted from the insertion of both an $[Fe(\eta^5\text{-}C_5H_5)]$ fragment and a carbon atom, presumably from a CO ligand, into the cage. A second reported example involved the irradiation of the $[Fe(\eta^5\text{-}C_5H_5)(CO)_2(\mu\text{-}4,5\text{-}C_2B_4H_7)]$ complex, which resulted in the formation of $[Fe(\eta^5\text{-}C_5H_5)(H)C_2B_4H_6]$ and $[Fe(\eta^5\text{-}C_5H_5)C_2B_4H_6]$ complexes as shown in Scheme 1.[7,8] The final example involved a photoinduced cyclo-insertion reaction of an alkyne into $B_4H_8Fe(CO)_3$ to yield several new carboranes.[6] Detailed pathway investigations and further photochemical studies beyond the initial work have not been reported for these systems.

In our previous work, we have reported on the photochemistry of the phosphino-substituted σ-metalated pentaborane complex, $[\mu\text{-}2,3\text{-}(P(C_6H_5)_3)\text{-}4\text{-}(Fe(\eta^5\text{-}C_5H_5)(CO)_2)B_5H_8]$ (**7**).[12] In this work, summarized in Scheme 2, we found that the photochemical reaction of **7** produced a new metallaborane complex **8** in very high yield.[12] This conversion was accompanied by the loss of a carbonyl ligand from the iron fragment, loss of a boron vertex from the cage, and a structural rearrangement. The subsequent reaction of compound **8** with silica gel was found to convert it into the new triboron complex **9** through the loss of an additional vertex boron atom and a second structural rearrangement. While many borane and metallaborane cage

Scheme 2. Photochemical Reactions of the Iron-Substituted Phosphinopentaborane Cluster, $[\mu\text{-}2,3\text{-}(P(C_6H_5)_3)\text{-}4\text{-}(Fe(\eta^5\text{-}C_5H_5)(CO)_2)B_5H_8]$ (**7**)[12] (Fp Indicates the $[Fe(\eta^5\text{-}C_5H_5)(CO)_2]$ Subunit and Cage Hydrogen Atoms Have Been Omitted for Clarity)

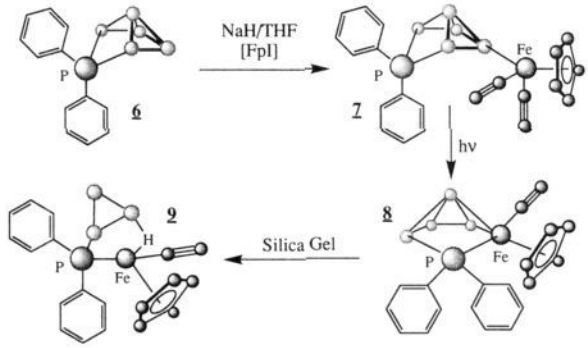

expansion reactions are known,[13−15] there are relatively few examples of a single boron vertex removal process from a small borane cluster (excluding carboranes and metallacarboranes) and none in which this process has been carried out sequentially to remove two vertices.[16−20] Importantly, this system provided extremely high selectivity for a single product pathway. This particular feature of cluster photochemical studies would be anticipated to yield meaningful results and interpretations of the mechanistic studies of accessible cluster photochemical pathways. An understanding of these pathways should provide very valuable insights into the overall chemistry of cluster molecules in general.

Several high-intensity photolytic and photodissociation studies of pure boranes, such as diborane(6), pentaborane(9), and decaborane(14), have been previously reported.[16−23] Gaseous pentaborane(9) was found to dissociate into B_4H_6 and BH_3 upon UV laser irradiation at 193 nm.[21] The initial products from the irradiation of pentaborane(9) at 253.7 nm in the presence of mercury, however, were proposed to be molecular hydrogen and B_5H_7.[24,25]

In the work reported here, we describe the effect of a photochemically generated unsaturated iron center on a σ-metalated pentaborane cluster. The photochemical transformations of $2\text{-}(Fe(\eta^5\text{-}C_5H_5)(CO)_2)B_5H_8$ (**1**) and $2,4\text{-}(Fe(\eta^5\text{-}C_5H_5)\text{-}(CO)_2)_2B_5H_7$ (**2**) were investigated in detail. The $Fe(\eta^5\text{-}C_5H_5)\text{-}(CO)_2$ moiety is typically readily decarbonylated with UV light to generate an unsaturated 16-electron iron center. Borane

(11) Randolph, C. L.; Wrighton, M. S. *Organometallics* **1987**, *6*, 365.
(12) Goodreau, B. H.; Orlando, L. R.; Spencer, J. T. *J. Am. Chem. Soc.* **1992**, *114*, 3827.
(13) Onak, T. In *Comprehensive Organometallic Chemistry*; Wilkinson, G., Stone, F. G. A., Abel, E., Eds.; Pergamon: Oxford, 1982; Chapter 5.4, p 411.
(14) Grimes, R. N. In *Comprehensive Organometallic Chemistry*; Wilkinson, G., Stone, F. G. A., Abel, E., Eds.; Pergamon: Oxford, 1982; Chapter 5.5.
(15) Grebenik, P. D.; Leach, J. B.; Green, M. L. H.; Walker, N. M. *J. Organomet. Chem.* **1988**, *345*, C31.
(16) Inkrott, K. E.; Shore, S. G. *J. Chem. Soc., Chem. Commun.* **1978**, 866.
(17) Spencer, J. T.; Grimes, R. N. *Organometallics* **1987**, *6*, 323.
(18) Grimes, R. N.; Beer, D. C.; Sneddon, L. G.; Miller, V. R.; Weiss, R. *Inorg. Chem.* **1974**, *13*, 1138.
(19) Maxwell, W. M.; Miller, V. R.; Grimes, R. N. *Inorg. Chem.* **1976**, *98*, 4818.
(20) Venable, T. L.; Grimes, R. N. *Inorg. Chem.* **1982**, *21*, 887.
(21) Irion, M. P.; Kompa, K. L. *J. Photochem.* **1987**, *37*, 233.
(22) Irion, M. P.; Seitz, M.; Kompa, K. L. *J. Mol. Spectrosc.* **1986**, *118*, 64.
(23) (a) Gaines, D. F.; McGaff, R. W.; Powell, D. R. *Inorg. Chem.* **1993**, *32*, 2612. (b) Mangion, M.; Ragaini, J. D.; Schmitkons, T. A.; Shore, S. G. *J. Am. Chem. Soc.* **1979**, *101*, 754. (c) Srivastava, D. K.; Rath, N. P.; Barton, L. *Organometallics* **1992**, *11*, 2263. (d) Edvenson, G. M.; Gaines, D. F.; Harris, H. A.; Campana, C. F. *Organometallics* **1990**, *9*, 401.
(24) Plotkin, J. S.; Astheimer, R. J.; Sneddon, L. G. *J. Am. Chem. Soc.* **1979**, *101*, 4155.
(25) Kline, G. A.; Porter, R. F. *Inorg. Chem.* **1980**, *19*, 447.

clusters offer the possibility that a photochemically generated unsaturated metal center attached to the cage could insert into borane cage, isomerize to a bridging position, or initiate further cluster rearrangements. Also investigated was the relationship between photochamical ligand dissociation and homolytic bond cleavage reactions in metallaboranes. The work reported here has initially focused upon the isolation and characterization of the products of these photochemical reactions in order to elucidate what types of transformations and mechanisms may be possible in the photochemistry of borane clusters.

Experimental Section

Physical Measurements. All NMR spectra were recorded on samples dissolved in $CDCl_3$ or THF-d_8 in 5 mm (o.d.) tubes. Boron (^{11}B) NMR spectra were recorded on either a Cryomagnetics CM-250 spectrometer operating at 80.26 MHz and equipped with a Brüker Aspect 3000 acquisition computer and pulse programmer or a General Electric GN-500 spectrometer operating at 160.45 MHz. Spectra were referenced to BBr_3 at +40.0 ppm (relative to $BF_3{\cdot}Et_2O$ at $\delta = 0.0$ ppm, with positive chemical shifts indicating downfield resonances) and recorded in both the ^1H coupled and decoupled modes. Typical ^{11}B NMR acquisition parameters employed were a relaxation delay of 1 s and a 90° pulse of 25 ms for the 160.45 MHz spectra. The 2D $^{11}B-^{11}B$ $\{^1H\}$ COSY NMR spectra, both the absolute value and pure phase versions, were obtained on either the CM-250 or the GN-500 spectrometer. Typically, a 90° pulse width of 15 to 25 ms was required on the CM-250 while the GN-500 required approximately twice this value. In most cases, a previously described absolute value mode COSY pulse sequence[26] was used to generate the t_1, t_2 data matrix (relaxation delay$-(\pi/2)-t_1-(\pi/2)-t_2$) in which t_1 was incremented by the inverse of the sweep width in the F_1 dimension and t_2 was the usual acquisition time in a 1D experiment. Typically, the t_1, t_2 matrix was collected as 128 × 256 data points, unless otherwise indicated. Data processing involved the application of a DC offset and first point correction, shifted sine bell apodization, zero filling (twice in t_1 and once in t_2), Fourier transformation, and a magnitude calculation to give the 512 × 512 2D $^{11}B-^{11}B$ COSY NMR spectrum.[27] Carbon (^{13}C) NMR spectra were recorded on a General Electric QE-300 spectrometer operating at 75.48 MHz. The spectra were referenced to $CDCl_3$ at $\delta = 77.0$ ppm or THF-d_8 at $\delta = 67.4$ ppm. Proton (^1H) NMR spectra were recorded on a General Electric QE-300 spectrometer operating at 300.15 MHz with chemical shifts referenced to an internal standard of tetramethylsilane at $\delta = 0.0$ ppm. Mass spectra were obtained on a Finnigan 4021 mass spectrometer using an ionization potential of between 11 and 30 eV. High-resolution mass spectra were recorded on a VG Analytical 7035 magnetic sector mass spectrometer at 30 eV. FT-IR spectra in the range of 400 to 4000 cm^{-1} were measured on a Mattson Galaxy 2020 spectrometer and were referenced to the 1601.8-cm^{-1} band of polystyrene. All compounds were recorded as Nujol mulls sandwiched between NaCl or KBr plates. UV−vis spectra were recorded on a Hewlett Packard 8452 spectrometer. Elemental analyses were performed by the Schwarzkopf Microanalytical Laboratories, Woodside, NY.

Materials. All photochemical reactions were accomplished using a water cooled quartz immersion-well photochemical reactor (Ace No. 7841) with a Conrad-Hanovia 450W Hg vapor lamp light source (Ace No. 7825-34). An inert atmosphere was typically maintained in the reactor during the irradiations by a dry nitrogen purge. The starting materials, 2-($Fe(\eta^5\text{-}C_5H_5)(CO)_2)B_5H_8$ (**1**) and 2,4-$[Fe(\eta^5\text{-}C_5H_5)(CO)_2]_2B_5H_7$ (**2**), were prepared according to the procedures previously described.[28] Tetrahydrofuran (Fisher) was ACS reagent grade and was distilled under a dry nitrogen atmosphere from sodium metal/benzophenone onto sodium hydride for storage. Pentane (Fisher) was distilled from sodium metal under a dry nitrogen atmosphere. All solvents were degassed by repeated freeze−thaw cycles and finally stored *in vacuo*. Methylene chloride (Fisher) was dried and distilled directly from P_2O_5. Deuterated solvents were stored over 4 Å molecular sieves prior to use. Pentaborane(9) was taken directly from our laboratory stock. All other commercially available chemicals were used as received. Analytical thin-layer chromatography was conducted on 2.5 × 7.5 cm silica gel strips (1B-F, Baker) and conventional column chromatography was conducted with 230−400 mesh (ASTM) silica gel (EM Science).

[2-(η^5-C_5H_5)-2-(CO)-2-FeB_5H_8], (3). A solution of 3.40 g (14.2 mmol) of [2-($Fe(\eta^5\text{-}C_5H_5)(CO)_2)B_5H_8$] (**1**) in 75 mL of dry THF was syringed into a water cooled photochemical reactor (Ace No. 7841) with a quartz immersion well under a nitrogen atmosphere. The clear orange solution was irradiated for 31 h. During this time, the reaction solution changed from a clear orange to a clear red-brown color. The ^{11}B NMR resonances for the starting material were observed to slowly disappear while the generation and growth of a new set of peaks were observed during the photochemical reaction. The irradiation was terminated when the ^{11}B NMR resonances for starting material had completely disappeared and only product resonances were observed (along with some small (<5%) unidentified resonances). The new product, **3**, was formed in 63% yield by ^{11}B NMR integration. The solvent was removed *in vacuo* to give a red-brown oil. Purification of [$Fe(\eta^5\text{-}C_5H_5)(CO)B_5H_8$] (**3**) by vacuum sublimation at 40 °C and 10^{-4} Torr yielded 0.54 g (19% isolated yield). A significant amount of decomposition occurred during the sublimation purification process. Treatment of a sample of **3** in THF with either CO or PPh_3 showed no changes in the ^{11}B NMR spectrum. Anal. Calcd for $C_6H_{13}B_5FeO$: C, 33.28; H, 5.29. Found: C, 34.14; H, 6.21. Complete spectroscopic data for **3** are given in Table 1.

Photochemistry of 1 in Pentane. A solution of 0.118 g of **1** was dissolved in 20 mL of pentane and irradiated for 1 h under the conditions described above. The solvent was removed *in vacuo* to give a red-brown oil. The oil was extracted with $CDCl_3$ giving a red solution and leaving an insoluble tan residue. The ^{11}B NMR of the red solution showed that it contained no boron. Proton NMR of the red solution showed that $[Fe(\eta^5\text{-}C_5H_5)(CO)_2]_2$ was the only soluble product (^1H NMR: $\delta = 4.78$; lit. $\delta = 4.78$ ppm).

[4-($Fe(\eta^5\text{-}C_5H_5)(CO)_2$)-2-($\eta^5$-$C_5H_5$)-2-(CO)-2-$FeB_5H_7$] (4). A solution of 0.10 g (0.24 mmol) of [2,4-$(Fe(\eta^5\text{-}C_5H_5)(CO)_2)_2B_5H_7$] (**2**) in 20 mL of THF was irradiated for 30 min. During this time the original yellow solution became dark red in color. Analysis of the solution by ^{11}B NMR showed that ~50% of the starting material had been converted to a new product. The ratio of the major product to all other products was ~50:1 based on ^{11}B NMR integration. The solvent was vacuum distilled away from the reaction mixture leaving a dark red solid. Extraction of this solid with 2 × 10 mL of dry pentane followed by solvent removal yielded 0.03 g of **4** (64% yield based on 50% consumption of **2**). Samples of **4** isolated in this fashion were approximately ~90% pure based on ^1H and ^{11}B NMR. The impurity was mainly the starting material **2** with some $[Fe(\eta^5\text{-}C_5H_5)(CO)_2]_2$. Attempts to purify **4** by chromatography on silica gel or sublimation resulted in the complete decomposition of the sample. The complete spectroscopic data for **4** are given in Table 1.

Irradiation of [4-($Fe(\eta^5\text{-}C_5H_5)(CO)_2$)-2-($\eta^5$-$C_5H_5$)-2-(CO)-2-$FeB_5H_7$] (4). The irradiation of **4** (or the irradiation of **2** for longer periods of time) was found to result only in the formation of [2-$Fe(\eta^5\text{-}C_5H_5)$-

(26) (a) Goodreau, B. H.; Spencer, J. T. *Inorg. Chem.* **1992**, *31*, 2612. (b) Venable, T. L.; Hutton, W. C.; Grimes, R. N. *J. Am. Chem. Soc.* **1984**, *106*, 29. (c) Wang, Z.; Sinn, E.; Grimes, R. N. *Inorg. Chem.* **1985**, *24*, 826. (d) Brewer, C. T.; Swisher, R. G.; Sinn, E.; Grimes, R. N. *J. Am. Chem. Soc.* **1985**, *107*, 3558. (e) Gaines, D. F.; Edvenson, G. M.; Hill, T. G.; Adams, B. R. *Inorg. Chem.* **1987**, *26*, 1813. (f) Edvenson, G. M.; Gaines, D. F.; Harris, H. A.; Campana, C. F. *Organometallics* **1990**, *9*, 410. (g) Meina, D. G.; Morris, J. H.; Reed, D. *Polyhedron* **1986**, *5*, 1639. (h) Jacobsen, G. B.; Meina, D. G.; Morris, J. H.; Thomson, C.; Andrews, S. J.; Reed, D.; Welch, A. J.; Gaines, D. F. *J. Chem. Soc., Dalton Trans.* **1985**, 1645. (i) Fontaine, X. L. R.; Greenwood, N. N.; Kennedy, J. D.; MacKinnon, P. *J. Chem. Soc., Dalton Trans.* **1988**, 1785. (j) Howarth, O. W.; Jasztal, M. J.; Taylor, J. G.; Wallbridge, M. G. H. *Polyhedron* **1985**, *4*, 1461. (k) Hermanek, S.; Fusek, J.; Stibr, B.; Plesek, J.; Jelinek, T. *Polyhedron* **1987**, *6*, 1873. (l) Jelinek, T.; Stibr, B.; Mares, F.; Plesek, J.; Hemanek, S. *Polyhedron* **1987**, *6*, 1737. (m) Kester, J. G.; Huffman, J. C.; Todd, L. J. *Inorg. Chem.* **1988**, *27*, 4528. (n) Kang, S. O.; Carroll, P. J.; Sneddon, L. G. *Organometallics* **1988**, *7*, 772. (o) Little, J. L.; Whitesell, M. A.; Kester, J. G.; Folting, K.; Todd, L. J. *Inorg. Chem.* **1990**, *29*, 804. (p) Getman, T. D.; Deng, H.-B.; Hsu, L.-Y.; Shore, S. G. *Inorg. Chem.* **1989**, *28*, 3612. (q) Brewer, C. T.; Grimes, R. N. *J. Am. Chem. Soc.* **1985**, *107*, 3552.

(27) (a) James, T. L.; McDonald, G. G. *J. Magn. Reson.* **1973**, *11*, 58. (b) Levy, G. C.; Peat, I. R. *J. Magn. Reson.* **1975**, *18*, 500.

(28) (a) Fischer, M. B.; Gaines, D. F.; Ulman, J. A. *J. Organomet. Chem.* **1982**, *231*, 55. (b) Greenwood, N. N.; Kennedy, J. D.; Savory, C. G.; Staves, J.; Trigwell, K. R. *J. Chem. Soc., Dalton Trans.* **1978**, 237.

Table 1. Spectroscopic Data for Compounds **1**–**4**

compd	^{11}B data[a]	^{1}H data[a]	IR (cm^{-1})[b]	mass spectral data[c]
1	7.9 (s, B(2)), −10.6 (d, B(3,4), J_{BH} = 150 Hz), −14.3 (d, B(5), J_{BH} = 160 Hz), −48.5 (d, B(1), J_{BH} = 170 Hz)	−2.02 (br s, 2H, μBHB), −1.11 (br s, 2H, μBHB), 0.57 (q, 1H, BH, J_{BH} = 166.2 Hz), 2.56 (q, 3H, BH, J_{BH} = 167.5 Hz), 4.79 (s, 5H, C_5H_5)	3118 (w, ν_{CH}), 2581 (vs, ν_{BH}), 2005 (vs, ν_{CO}), 1947 (vs, ν_{CO}), 1776 (m), 1014 (m), 1002 (m), 966 (m), 883 (m), 835 (s), 640 (m)	240[d] (2.4; P+ envelope, $^{12}C_7{}^{1}H_{13}{}^{11}B_5{}^{56}Fe^{16}O_2$), 212 (25.9; P+ − CO envelope), 184 (28.6; P+ − 2CO envelope)
2	2.7 (s, B(3,5)), −7.8 (d, B(2,4), J_{BH} = 133 Hz), −43.3 (d, B(1), J_{BH} = 168 Hz)	−1.9 (br, 2H, μBHB), −0.8 (br, 2H, μBHB), 0.9 (br q, 1H, BH), 2.7 (br q, 3H, BH), 4.95 (5H, C_5H_5)	2565 (w, ν_{BH}), 2510 (w, ν_{BH}), 1996 (vs, ν_{CO}), 1936 (vs, ν_{CO}), 1261 (m), 1194 (w), 1093 (m), 1026 (m), 925 (w), 800 (m), 744 (w), 694 (m), 644 (m), 590 (w)	415[d] (1.0; P+ envelope, $^{12}C_{14}{}^{1}H_{17}{}^{11}B_5{}^{56}Fe_2{}^{16}O_4$), 386 (5.0; P+ − CO envelope), 358 (8.8; P+ − 2CO envelope), 330 (9.0; P+ − 3CO envelope), 301 (46.0; P+ − 4CO, H_2 envelope)
3	76.0 (d, B(2,3), J_{BH}= 158 Hz), 10.9 (d, B(4,5), J_{BH} = 158 Hz), −45.5 (d, (B)1, J_{BH} = 129 Hz)	−1.79 (q, 1H, BH (apical)), 0.58 (br s, 1H, μBHB), 1.33 (br s, 2H, μBHB), 3.7 (q, 2H, BH (basal)), 4.91 (s, 5H, C_5H_5), 8.1 (q, 2H, BH (basal))	3116 (w, ν_{CH}), 2565 (s, ν_{BH}), 2526 (s, ν_{BH}), 1940 (s, ν_{CO}), 1415 (m), 1360 (m), 1313 (m), 1016 (w), 1002 (w), 923 (m), 892 (m), 831 (m), 694 (m), 565 (m), 536 (m)	208 (found 18.5, calcd 4.6; P^+ envelope), 209 (found 27.0, calcd 18.2; P^+ envelope), 210 (found 64.9, calcd 53.9; P^+ envelope), 211 (found 100.0, calcd 100.0; P^+ envelope $^{12}C_6{}^{1}H_{13}{}^{11}B_5{}^{56}Fe^{16}O$), 212 (found 83.6, calcd 85.3; P^+ envelope), 213 (found 12.2, calcd 7.8; P^+ envelope)
4	74.9 (d, B(3), J_{BH} = 139 Hz), 73.5 (d, B(6), J_{BH} = 135 Hz), 35.7 (s, B(4)), 11.7 (d B(5), J_{BH} = 144 Hz), −39.4 (d B(1), J_{BH} = 139 Hz)	4.80 (s, C_5H_5), 4.83 (s, C_5H_5)	2538 (w, ν_{BH}), 2510 (w, ν_{BH}), 2008 (s, ν_{CO}), 1955 (s, ν_{CO}), 1941 (s, ν_{CO}), 1791 (w), 1261 (m), 1018 (m), 802 (w), 644 (w), 592 (w)	385 (found 35.8, calcd 23.7; P^+ envelope), 386 (found 63.6, calcd 57.8; P^+ envelope), 387 (found 100.0, calcd 100.0; P^+ envelope $^{12}C_{13}{}^{1}H_{17}{}^{11}B_5{}^{56}Fe_2{}^{16}O_3$), 388 (found 88.2, calcd 90.3; P^+ envelope), 389 (found 19.2, calcd 16.7; P^+ envelope), 390 (found 9.1, calcd 2.4; P^+ envelope), 359 (65.8, P^+ − CO), 331 (100.0, P^+ − 2CO)

[a] NMR data in $CDCl_3$. Abbreviations: s = singlet, d = doublet, q = quartet, m = multiplet, unres = unresolved coupling, br = broad. [b] Nujol mull. Abbreviations: vs = very strong, s = strong; m = medium; w = weak; sh = shoulder; br = broad. [c] Relative intensities are given with the largest peak in the P^+ envelope normalized to 100.0%. The calculated values are based on natural isotopic abundances which are normalized to the most intense peak in the envelope. [d] Mass spectral data from ref 28.

$(CO)B_5H_8]$ (**3**) and $[Fe(\eta^5\text{-}C_5H_5)(CO)_2]$, which were identified completely by spectroscopic techniques (Table 1). No other products were observed.

[3-(Fe(η^5-C_5H_5)(CO)$_2$)-2-(η^5-C_5H_5)-2-(CO)-2-FeB$_5$H$_7$] (5). A sample of complex **4** was allowed to stand for 48 h under vacuum in a sealed flask. Upon redissolving the sample in pentane, the ^{11}B NMR spectrum revealed that the sample contained a ~1:2 mixture of unreacted **4** and a new complex, [2-(Fe(η^5-C_5H_5)(CO))-3-(Fe(η^5-C_5H_5)(CO)$_2$)B_5H_7] (**5**) [^{11}B NMR, pentane; δ 118.9 (s, J_{BH} = 73.4 unresolved coupling), 13.0 (d, J_{BH} = 114 Hz), 6.1 (d, J_{BH} = 114 Hz), −42.3 (d, J_{BH} = 139 Hz)]. Attempts to purify **5** by chromatography, sublimation, and other methods resulted in the complete decomposition of the sample.

X-ray Crystallography of 3. A 0.2 × 0.2 × 0.2 mm red crystal of pure **3** was grown by vacuum sublimation of complex **3** at 10^{-4} Torr and 40 °C. The crystal was mounted in a 0.2 mm Lindemann capillary tube and sealed under an inert atmosphere. All measurements were made on a Rigaku AFC5S diffractometer using graphite monochromated Mo Kα radiation (λ = 0.71073 Å). Cell constants and an orientation matrix for the data collection were obtained from a least-squares refinement using 25 centered high-angle reflections in the range of 25.15° < 2θ < 28.70°. Based on the systematic absences of $0kl$, $k + l \neq 2n$ and $hk0$, $h \neq 2n$ and the successful structural solution, the space group was uniquely determined to be *Pnma*. Data were collected at room temperature using a ω–2θ scan technique 2$\theta \leq$ 69.9°. Three reference reflections were monitored every 100 reflections during data collection and no significant variation in intensity occurred. Data reduction of 1908 unique measured reflections resulted in 959 reflections with $I > 3\sigma(I)$ which were used for the structure refinement (reflection/parameter = 9.99). The position of the iron atom was determined from a Patterson synthesis and the remaining non-hydrogen atoms were located by application of direct methods to generate a trial structure.[29,30] The non-hydrogen atoms were refined anisotropically. The hydrogen atoms were then located on a difference map and refined isotropically. The final cycle of a full-matrix least-squares refinement converged with $R = [(\sum(|F_o| - |F_c|)^2/\sum(F_o)^2]^{1/2} = 0.036$ and $R_w = [(\sum w(|F_o| - |F_c|)^2/\sum w(F_o)^2]^{1/2} = 0.037$. The final structure was plotted using the TEXSAN[31] graphics programs, including PLUTO[32] and ORTEP.[33] The crystallographic data, selected bond lengths, and selected bond angles for **3** are given in Tables 2–4. All atom coordinates, anisotropic thermal parameters, bond distances and angles involving both non-hydrogen and hydrogen atoms, intermolecular distances, PLUTO diagrams for **3**, and a listing of observed and calculated structure factors are available as supporting information.

Results and Discussion

As presented above, the fields of organic and organometallic photochemistry are relatively well developed areas of investigation. In an attempt to build upon the detailed information known in these related fields with investigations of main group cluster photochemical processes, we have first explored the photochemistry of organometallic derivatives of borane clusters related to the well-known $[Fe(\eta^5\text{-}C_5H_5)(CO)_2R]$ complexes (R = alkyl or aryl).

Two $[Fe(\eta^5\text{-}C_5H_5)(CO)_2]$-substituted pentaborane clusters have been previously reported in the literature, [2-(Fe(η^5-C_5H_5)-(CO)$_2$)B_5H_8] (**1**) and [2,4-(Fe(η^5-C_5H_5)(CO)$_2$)$_2B_5H_7$] (**2**).[28] These compounds provide valuable models for cluster photochemical investigations. As anticipated, compounds **1** and **2** were found to have intense ultraviolet absorptions (Figure 1) with their color arising primarily from the tailing of an

(29) Calbrese, J. C. PHASE. Patterson Heavy Atom Solution Extractor. Ph.D. Dissertation, University of Wisconsin, Madison, WI, 1972.

(30) Beurskens, P. T. DIRDIF. Direct Methods for Difference Structures. Technical Report. 1984/1; Crystallography Lab.; Toernooiveld, 6525 Ed. Nijmegen, The Netherlands.

(31) TEXSAN. Texray Structure Analysis Package, Molecular Structure Corp., 1985.

(32) Motherwell, S.; Clegg, W. pluto. Program for plotting molecular and crystal structures; University of Cambridge, England, 1978.

(33) Johnson, C. K. ORTEPII. Report ORNL-5138; Oak Ridge National Laboratory: Oak Ridge, TN, 1976.

Table 2. Crystallographic Data for **3**

chemical formula	$C_6H_{13}B_5FeO$
formula weight	211.07
crystal system	orthorhombic
space group	*Pnma* (No. 62)
temp (K)	298
cell dimens (at 298 K)	
a (Å)	14.889(1)
b (Å)	9.4560(9)
c (Å)	7.2838(9)
V (Å^3)	1025.5(3)
Z (molecules/cell)	4
λ(Mo Kα) (Å)	0.71073
diffractometer	Rigaku AFC5S
ρ_{calcd} (g cm^{-3})	1.367
μ (cm^{-1})	14.17
transmission coeff	
Ψ	0.8732−1.0000
Ψ_{av}	0.9580
R	0.039
R_w	0.037
total no. of reflcns	1908
no. of reflcns with $I > 3\sigma(I)$	959
no. of variables	96
$2\theta_{max}$ (deg)	69.9
goodness of fit	1.23
max shift/error in final cycle	0.00

Table 3. Intramolecular Bond Distances for **3**[a]

bond	distance[a]	bond	distance[a]
Fe−C(1)	1.728(4)	C(11)−C(12)	1.404(4)
Fe−C(11)	2.106(4)	C(12)−C(13)	1.402(4)
Fe−C(12)	2.118(3)	C(13)−C(14)	1.417(7)
Fe−C(13)	2.100(3)	B(2)−B(5)	1.777(5)
Fe−B(1)	2.161(4)	B(1)−B(2)	1.738(4)
Fe−B(2)	1.968(4)	B(1)−B(4)	1.767(5)
O(1)−C(1)	1.146(5)	B(4)−B(5)	1.814(8)
C(11)−H(11)	0.95(4)	B(2)−H(2)	1.07(3)
C(12)−H(12)	0.94(3)	B(5)−H(8)	1.19(3)
C(13)−H(13)	0.94(3)	B(5)−H(5)	1.10(3)
		B(5)−H(7)	1.25(3)
		B(1)−H(1)	1.07(4)

[a] Distances are in angstroms. The estimated standard deviations in the least significant figure are given in parentheses.

Table 4. Selected Intramolecular Bond Angles for **3**[a]

atoms	angle[a]	atoms	angle[a]
C(1)−Fe−C(11)	162.3(2)	C(13)−Fe−B(1)	151.0(1)
C(1)−Fe−C(12)	130.2(1)	C(13)−Fe−B(2)	114.1(1)
C(1)−Fe−C(13)	98.4(2)	B(1)−Fe−B(2)	49.5(1)
C(1)−Fe−B(1)	102.7(2)	Fe−C(1)−O1	178.1(4)
C(1)−Fe−B(2)	84.7(1)	Fe−C(11)−C(12)	71.1(2)
C(11)−Fe−C(12)	38.8(1)	Fe−C(12)−C(13)	69.9(2)
C(11)−Fe−B(1)	94.9(2)	C(11)−C(12)−C(13)	107.4(3)
C(11)−Fe−B(2)	107.2(1)	Fe−C(13)−C(13)	70.28(9)
C(12)−Fe−B(1)	112.6(1)	Fe−B(1)−B(2)	59.5(2)
B(2)−B(1)−B(5)	60.9(2)	Fe−B(1)−B(5)	107.5(2)
Fe−B(2)−B(1)	71.0(2)	B(2)−B(1)−B(2)	109.6(3)
B(1)−B(2)−B(5)	60.3(2)	Fe−B(2)−B(5)	115.9(2)
B(1)−B(5)−B(2)	58.7(2)		

[a] Angles are in degrees. Estimated standard deviations in the least significant figure are given in parentheses.

absorption band at ~330 nm into the visible region. This absorption is typical of many [Fe(η^5-C_5H_5)$(CO)_2$R] complexes (where R = alkyl, aryl, and halogen) and has been attributed to transitions involving the π^* Fe−R antibonding orbital.[3] A second stronger group of bands occurs in the UV region for complexes **1** and **2** at 250−290 nm. These latter bands are a mixture of absorptions arising principally from the aromatic and borane substitutents of the complexes.[21,22,34]

The LUMO for [Fe(η^5-C_5H_5)$(CO)_2$R] complexes is usually a M−CO antibonding orbital while the HOMO is typically

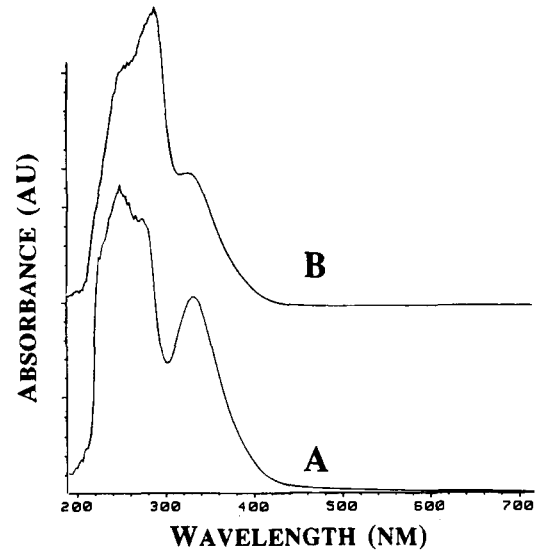

Figure 1. Ultraviolet−visible spectra for; (A) [2-(Fe(η^5-C_5H_5)$(CO)_2$)-B_5H_8] (**1**) and (B) [2,4-(Fe(η^5-C_5H_5)$(CO)_2)_2B_5H_7$] (**2**) complexes.

Fe−R antibonding in nature. Thus, ultraviolet photochemical excitation would be anticipated to effectively increase the strength of the M−R interaction while weakening the M−CO bond leading to CO dissociation and the generation of a transient 16-electron unsaturated iron intermediate. These expectations have been previously shown to be consistent with both calculations and photoelectron spectra for a variety of [Fe(η^5-C_5H_5)-$(CO)_2$R] complexes.[35] By analogy with these [Fe(η^5-C_5H_5)-$(CO)_2$R] complexes, the absorption of ultraviolet radiation by compounds **1** and **2** is likely to similarly involve the population of an Fe−CO antibonding orbital, leading to ligand dissociation and the generation of an unsaturated iron center directly attached to the borane cage.

Upon ultraviolet irradiation of complex **1** in THF solution, a new complex, identified as [2-(η^5-C_5H_5)-2-(CO)-2-FeB_5H_8] (**3**), was obtained in 63% yield. In this photoinitiated process, a decarbonylation reaction of the organometallic fragment occurs, presumably followed by an insertion of the iron center into the basal plane of the borane cluster. The reaction was found to be chemically irreversible. For example, when compound **3** was treated with either CO or PPh_3, no reaction was observed and **3** was recovered quantitatively. The spectroscopic characterization of complex **3** (Table 1) is consistent with a pentagonal pyramidal structure in which an Fe(η^5-C_5H_5)(CO) unit occupies a vertex in the basal plane of the FeB_5 cage. This reaction is summarized in Scheme 3.

The FT-IR spectrum for complex **3** showed only a single CO stretch, consistent with the loss of one carbonyl group from the starting complex **1**. The ^{1}H NMR of the new complex showed resonances for the terminal protons of the borane cage as distinct boron-coupled quartets for the three types of terminal B−H protons in a 1:2:2 ratio [1 apical BH:4 basal BH]. The bridging μ-B−H−B protons appeared as broad resonances and those attributed to the η^5-cyclopentadienyl group of the organometallic fragment were observed at 4.90 ppm (relative intensity of 1:2:5, respectively). The ^{11}B NMR spectrum of the new complex consisted of three resonances with an intensity ratio of 2:2:1. Each of these resonances were observed as proton-coupled doublets which collapsed into sharp singlets upon proton decoupling. The ^{11}B NMR spectrum for **3** is similar to those

(34) Silverstein, R. M.; Bassler, G. C.; Morrill, T. C. *Spectroscopic Identification of Organic Compounds*; John Wiley and Sons: New York, 1981; p 308.

(35) Lichtenberger, D. L.; Fenske, R. F. *J. Am. Chem. Soc.* **1976**, *98*, 50.

Scheme 3. Photochemical Interconversions and Transformations of Iron-Substituted Pentaborane Clusters [2-(Fe(η^5-C_5H_5)$(CO)_2$)B_5H_8] (**1**) and [2,4-(Fe(η^5-C_5H_5)$(CO)_2$)$_2B_5H_7$] (**2**) (Fp Indicates the [Fe(η^5-C_5H_5)$(CO)_2$] Subunit and Cage Hydrogen Atoms Have Been Omitted for Clarity)

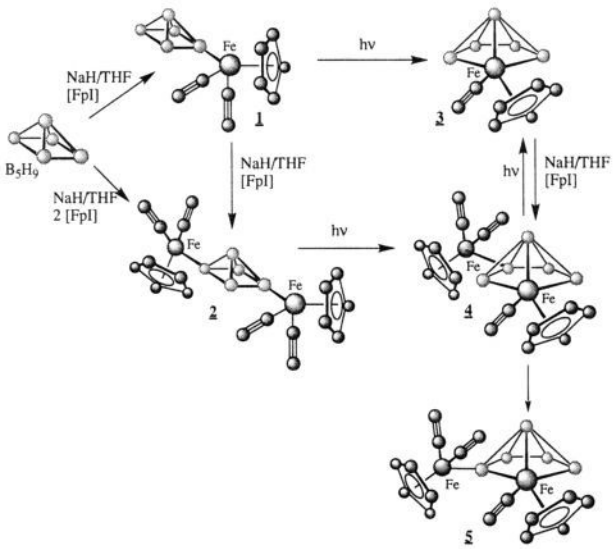

observed for the other known iron-inserted *nido*-pentaborane derivatives, [2-(Fe(η^5-C_5H_5))B_5H_{10}][36,37] (**10**) and [2-(Fe$(CO)_3$)-B_5H_9][23b,38,39] (**11**), shown in Figure 2. Compound **10** was prepared in very low yield from the reaction of $C_5H_5^-$ with $FeCl_2$ and *nido*-$B_5H_8^-$ (2.5% yield) while compound **11** was similarly formed in low yield from the thermal reaction (220 °C) of $Fe(CO)_5$ with *nido*-B_5H_9 (5% yield). The unusually large downfield shifted peak (δ = +76.0 ppm) in the ^{11}B NMR spectrum of **3** was assigned to the two basal boron atoms directly coordinated to the Fe(η^5-C_5H_5)(CO) unit. Analogous resonances for complexes **10** and **11** at room temperature were observed at +44.4 and +46.0 ppm. The significantly larger downfield shift for the boron atoms in complex **3** in comparison with complexes **10** and **11** may be due, in part, to the apparent lack of bridging μ-B−H−Fe interactions in complex **3**.

The spectroscopic structural assignment of **3** was verified by a single-crystal X-ray analysis of the complex. The molecular structure and numbering scheme for complex **3** is shown in Figure 3. In the structure, all the hydrogen atoms were located and refined without difficulty. Selected bond lengths and angles are given in Tables 3 and 4, respectively. As proposed based upon the spectroscopic data, the structure of **3** consists of a pentagonal-pyramidal structure in which the iron atom is bound to one carbonyl ligand, an η^5-cyclopentadienyl ring, and the borane cage through three boron vertices. The iron atom is located slightly below the cage's basal plane (0.34 Å). The observed Fe−B(2,3) distances for **3** were found to be slightly shorter (1.97 Å) than those found in the analogous [$N(C_4H_9)_4$]-[2-Fe$(CO)_3B_5H_9$] (2.08 and 2.13 Å)[23b] and related [μ-(Fe$(CO)_4B_7H_{12}$]$^-$ (2.22 and 2.20 Å)[39] complexes, again presumably due to the absence of any μ-Fe−H−B interactions in complex **3**. The Fe−C(carbonyl) bond distance of 1.723(5) Å in **3** was also found to be slightly shorter than other similar bond distances in iron carbonyl complexes (av Fe−$C_{(terminal)}$

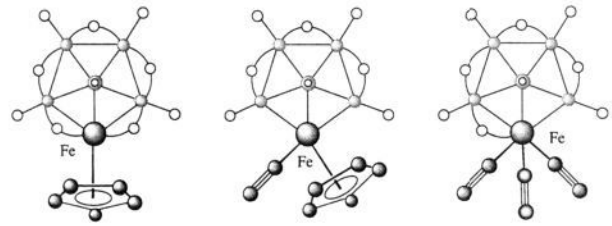

Figure 2. Apical view of complexes [2-(η^5-C_5H_5)-2-(CO)-2-FeB_5H_8] (**3**), [2-(Fe(η^5-C_5H_5))B_5H_{10}][36,37] (**10**), and [2-(Fe$(CO)_3$)B_5H_9][23b,38,39] (**11**) (small open circles in the figure represent hydrogen atoms).

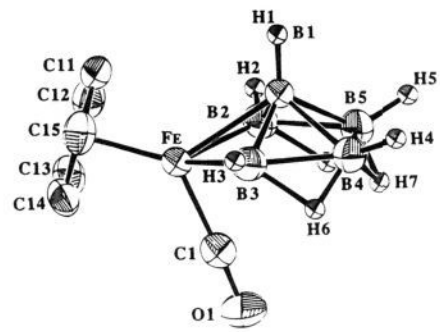

Figure 3. ORTEP drawing of [2-(η^5-C_5H_5)-2-(CO)-2-FeB_5H_8] (**3**) showing the atomic numbering scheme. The thermal ellipsoids are drawn at the 50% probability level. The hydrogen atoms of the C_5H_5 ring have been omitted for clarity.

ranging from ca. 1.74 to 1.82 Å).[40] The structure of **3** represents the first crystallographically characterized neutral *nido*-ferrahexaborane cluster to be reported, although the structure of the closely related [$N(C_4H_9)_4$][2-(Fe$(CO)_3$)B_5H_9] complex has been crystallographically determined.[23b] The observed X-ray structure of complex **3** can be best understood in terms of both the polyhedral skeletal electron pair theory (psept)[41] and the Effective Atomic Number (EAN)[42] constructs for electron counting. In the psept counting scheme, the Fe(η^5-C_5H_5)(CO) fragment contributes three electrons to the cage bonding, the five BH fragments contribute a total of ten electrons and the three μ-B−H−B bridging protons contribute three electrons for a total of 16 skeletal electrons. Thus, compound **3** is anticipated to display a six-vertex, 16-electron [$2n$ + 4] *nido*-cluster structure, which was observed crystallographically. Using the EAN scheme, the iron center (8-electron core) completes an 18-electron closed-shell configuration by the coordination of one CO ligand (2-electron donor), a cyclopentadienyl group (5-electron donor), and the pentaborane cage (3-electron donor).

In the attempted photochemical preparation of **3** in pentane rather than in THF, the dimeric [Fe(η^5-C_5H_5)$(CO)_2$]$_2$ complex was the only identifiable product in solution. The only boron-containing material isolated was an insoluble tan solid. This observation suggests that homolysis of the iron−boron bond occurred under these conditions rather than the previously observed decarbonylation reaction. In this iron−cage homolytic bond fission process, the initially photogenerated [Fe(η^5-C_5H_5)-$(CO)_2$]$^\bullet$ and $^\bullet$[B_5H_8] products would be expected, based upon previous work with the [Fe(η^5-C_5H_5)$(CO)_2(CH_2C_6H_5)$] complex,[9] to combine to give [Fe(η^5-C_5H_5)$(CO)_2$]$_2$ and $(B_5H_8)_2$. Since only [Fe(η^5-C_5H_5)$(CO)_2$]$_2$ was observed as a soluble

(36) Weiss, R.; Grimes, R. N. *Inorg. Chem.* **1979**, *18*, 3291.
(37) Weiss, R.; Grimes, R. N. *J. Am. Chem. Soc.* **1977**, *99*, 8087.
(38) Shore, S. G.; Ragaini, J. D.; Smith, R. L.; Cottrell, C. E.; Fehlner, T. P. *Inorg. Chem.* **1979**, *18*, 670.
(39) Brint, P.; Pelin, W. K.; Spalding, T. R. *J. Chem. Soc., Dalton Trans.* **1981**, 546.
(40) Gress, M. E.; Jacobson, R. A. *Inorg. Chem.* **1973**, *12*, 1746.
(41) (a) Mingos, D. M. P. In *Inorganometallic Chemistry*; Fehlner, T. P., Ed.; Plenum: New York, 1992; Chapter 4. (b) Wade, K. *Adv. Inorg. Chem. Radiochem.* **1976**, *18*, 1.
(42) Collman, J. P.; Hegedus, L. S.; Norton, J. R.; Finke, R. G. *Principles and Applications of Organotransition Metal Chemistry*; Univesity Science: Mill Valley, CA 1987.

Scheme 4. Fe−Cage Homolytic Bond Fission and Fe−CO Dissociation/Cage Insertion Reactions in the Photolysis of [2,4-(Fe(η^5-C_5H_5)(CO)$_2$)$_2B_5H_7$] (**2**).

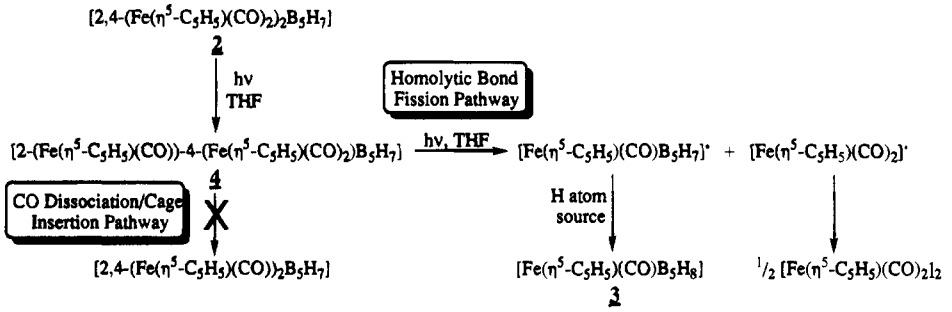

product, it appears that the borane radical is sufficiently unstable such that it decomposes into an insoluble product before it can be spectroscopically detected. The observation of the homolytic bond fission reaction in pentane suggests that the THF solvent is important in the overall reaction and might form an intermediate complex, such as [Fe(η^5-C_5H_5)(CO)(THF)B_5H_8], leading to the formation of **3**.

In light of the exceptionally clean photochemical transformation of complex **1** into complex **3**, an investigation of the photochemistry of the closely related bis-σ-metalated pentaborane complex, [2,4-(Fe(η^5-C_5H_5)(CO)$_2$)$_2B_5H_7$] (**2**), was begun. If the two iron organometallic fragments in complex **2** could undergo independent photoinitiated insertion processes, it might be possible to isolate a new Fe_2B_5 cluster.

Upon ultraviolet irradiation of complex **2**, a single new iron insertion product, [4-(Fe(η^5-C_5H_5)(CO)$_2$)-2-(η^5-C_5H_5)-2-(CO)-2-FeB_5H_7] (**4**), was isolated. The course of the photoreaction was monitored by ^{11}B NMR and the irradiation was continued until half of the starting material was consumed leaving only complexes **2** and **4** present in solution. The product **4** was separated from the starting material by repeated extractions with pentane (**4** was the more soluble component in pentane). The complete purification of complex **4** was not possible since very small amounts of [Fe(η^5-C_5H_5)(CO)$_2$]$_2$ remained after all purification attempts, including multiple extractions, recrystallization attempts, sublimation, chromatography, and other separation techniques. Silica gel chromatography of **4** resulted in its complete and rapid decomposition on the column.

The structural assignment of complex **4** was based on ^{11}B NMR (both 1D and 2D ^{11}B−^{11}B {^{1}H} COSY NMR experiments), ^{1}H NMR, FTIR, and mass spectroscopy. The proposed structure for complex **4** is shown in Scheme 3. The cage structure consists of a pentagonal FeB_5 pyramidal cluster similar to that observed for compound **3**. In compound **4**, however, there is an additional terminally-bound Fe(η^5-C_5H_5)(CO)$_2$ group σ-bound to one of the boron vertices which is not adjacent to the inserted iron center. The ^{11}B NMR spectrum of **4** consisted of five resonances of equal relative intensity. The resonance at 35.7 ppm was observed as a singlet while all of the other resonances were proton-coupled doublets which collapsed into singlets in the {^{1}H}^{11}B spectrum. The downfield ^{11}B NMR resonances at 74.9 and 73.5 ppm are assigned to the basal boron atoms adjacent to one inserted iron atom (B2,3). Their downfield shift is very similar in magnitude to that observed for the corresponding boron atoms in complex **3** (76.0 ppm). The only singlet resonance in the proton-coupled spectrum, at 35.7 ppm, is assigned to a basal boron atom σ-bound to a Fe(η^5-C_5H_5)(CO)$_2$ group (B4). The resonance at 11.7 ppm was assigned to the only remaining basal BH group in the pentagonal FeB_5 cluster (B5). Finally, the most upfield resonance was assigned to the apical boron atom (B1).

Two-dimensional NMR has proven to be a particularly powerful tool in confirming structural relationships in borane clusters.[23b,26] The 2D ^{11}B−^{11}B {^{1}H} COSY NMR spectrum of **4** (supporting information) displayed cross-peak connectivities consistent with the proposed structure. 2D correlations were clearly observed between the −39.4 ppm boron resonance (apical) and all of the other resonances; however, no correlations were observed between the basal boron resonances. The absence of cross peaks between the basal boron resonances is fully consistent with previous work where, in general, it has been observed that boron−boron 2-center−2-electron (2c−2e$^-$) bonds provide strong cross peaks while cross peaks arising from coupling through μ-B−H−B 3-center−2-electron (3c−2e$^-$) bonds (μ-$B_{(basal)}$−H−$B_{(basal)}$ in **4**) give either very weak or entirely missing cross peaks.[26] The observation of a cross peak in the 2D experiment requires the localization of significant electron density between correlated nuclei, since scalar coupling is propagated primarily through the bonding electrons. The development of cross peaks in the 2D spectrum also is greatly affected by the T_1 values for the coupled nuclei. The cross-peak intensity is, in general, attenuated when T_1 values are very small with respect to the reciprocal of J_{BB} (i.e., when $T_1 \ll (2\pi J)^{-1}$).[26c,43] Cross-peak intensities arising from μ-B−H−B interactions are typically very low because of the reduction of electron density localized between these basal boron atoms (very small J_{BB} values).[26a] Also contributing to the absence of basal−basal cross peaks in the 2D spectrum for metallaboranes are the very short spin−lattice relaxation times for the basal resonances for these complexes.[26] In the 2D spectra for the parent complexes, **1** and **2**, cross peaks between the apical and basal boron atoms were observed while no cross peaks were found between B(2,3) and B(4,5) atoms,[26] similar to that observed for complex **4**.

As anticipated, the ^{1}H NMR for **4** revealed two different types of cyclopentadienyl rings at (δ) 4.80 and 4.83 ppm, and the FT-IR data showed the presence of three carbonyl groups, clearly indicating the presence of two inequivalent organometallic iron units. The mass spectrum consisted of a parent envelope centered around 388 m/e$^-$ which corresponds well with the intensities calculated for the natural isotopic abundances in **4** ($C_{13}H_{17}B_5Fe_2O_3$). Thus, the only structure consistent with these data is that shown in Scheme 3.

Upon the extended UV irradiation of either complex **2** or **4**, the only products were the dimeric [Fe(η^5-C_5H_5)(CO)$_2$]$_2$ complex and the previously characterized complex **3**. These products apparently arise from the light-induced fission of a terminal σ-iron−cage bond as summarized in Scheme 4. The dimeric [Fe(η^5-C_5H_5)(CO)$_2$]$_2$ would be expected to form through a radical coupling process of the initially generated [Fe(η^5-C_5H_5)(CO)$_2$]· species. The other expected coupling product, [(Fe(η^5-C_5H_5)(CO))B_5H_7]$_2$, was not observed, but rather the formation of complex **3** was found to be the boron-containing

(43) (a) Stampf, E. J.; Garber, A. R.; Odom, J. D.; Ellis, P. D. *J. Am. Chem. Soc.* **1976**, *98*, 6550. (b) Weiss, R.; Grimes, R. N. *J. Am. Chem. Soc.* **1978**, *100*, 1401.

product. Complex **3** presumably forms through the extraction a hydrogen atom by the intermediate radical [2-(η^5-C_5H_5)-2-(CO)-2-FeB_5H_7]• complex. It seemed possible that such a borane radical species might be stable enough to allow its detection by ESR because of the electron delocalization within the cluster. ESR spectra of the THF solution immediately after irradiation of **2**, however, were unsuccessful in detecting any stable radical species. Homolytic fission of the Fe−R bond in [Fe(η^5-C_5H_5)$(CO)_2(CH_2C_6H_5)$] has been previously reported[10] but was found to be in competition with the CO dissociation pathway.[9] In this organometallic system, the CO dissociative process was found to occur with a much greater quantum efficiency than the homolytic Fe−R bond cleavage reaction. Even though the CO dissociative pathway was found to be a much more efficient process (10:1 for dissociation−fission), the observed room temperature products were predominately from the homolytic pathway, [Fe(η^5-C_5H_5)$(CO)_2]_2$ and $(C_6H_5CH_2)_2$. Variations in the observed product distribution from the two competing pathways as a function of temperature, however, were readily accounted for by considering the facile reversibility of the CO dissociative process and the presence or absence of a suitable ligand to intercept the coordinatively unsaturated intermediate. Thus, at higher temperatures, the reversible loss of CO coupled with the irreversibility and small but finite quantum yield for the Fe−R bond cleavage reaction accounted for the observed product distributions. It is unclear, however, in the apparent homolytic bond fission process in the conversion of complex **4** into **3** whether both CO dissociative and iron−cage bond fission pathways occur, albeit with vastly different quantum efficiencies as in the case of the [Fe(η^5-C_5H_5)$(CO)_2$-$(CH_2C_6H_5)$] complex, or whether the bond fission process occurs solely. It seems reasonable to suggest, however, that a similar competition between the two possible pathways is in operation in the photolysis of complex **4**.

After letting the reaction mixture stand under vacuum at room temperature, a new compound, [3-(Fe(η^5-C_5H_5)$(CO)_2$)-2-(η^5-C_5H_5)-2-(CO)-2-FeB_5H_7] (**5**), was isolated from the reaction mixture for the photochemical generation of complex **4**. The ^{11}B NMR of this extract showed the presence both **4** and **5** in a 1:2 ratio. The complete purification of complex **5** was not possible since a small amount of complex **4** remained in the samples after all purification attempts, including multiple extractions, recrystallization attempts, sublimation, chromatography, and other techniques. As with complex **4**, the silica gel chromatography of **5** resulted in its complete and rapid decomposition on the column. The structure of complex **5**, shown in Scheme 3, was unambiguously assigned spectroscopically. The rather unusual chemical shifts observed in the ^{11}B NMR of **5** lead to a structure in which the exopolyhedral [Fe(η^5-C_5H_5)$(CO)_2$] group is bound to the boron atom closest to the inserted iron atom. In the ^{11}B NMR spectrum, five peaks of equal intensity were observed over a range from 118.9 to −42.3 ppm. A resonance at 73.4 ppm, while rather broad from unresolved proton coupling (J_{BH}), did narrow significantly upon ^{1}H decoupling. The proposed structure of complex **5** consists of a FeB_5 pentagonal pyramid in which there is an additional terminally-bound Fe(η^5-C_5H_5)$(CO)_2$ group σ-bound to a boron vertex adjacent to the inserted iron center. The resonance at 118.9 ppm was assigned to a boron atom adjacent to the inserted iron atom (B3) and attached to a terminally-bound Fe(η^5-C_5H_5)-$(CO)_2$ group. The combination of two metal moieties shifting electron density from a single boron atom would be expected to result in this rather large downfield chemical shift (δ = 118.9 ppm), well out of the "typical" range observed for ^{11}B NMR. Similar large positive shifts have been observed for "metal-rich" metallaborane complexes and it appears that this large shift is characteristic of strong, direct boron−iron interactions.[44] The resonance at 73.4 ppm was assigned to the other boron atom adjacent to the inserted iron atom but without the terminally-bound Fe(η^5-C_5H_5)$(CO)_2$ group (B6). Resonances at 13.0 and 6.1 ppm were assigned to the remaining basal BH vertices (B4,5) with the −42.3 ppm resonance assigned to the apical boron atom (B1). The mechanism for this transformation is unknown and currently under investigation in our laboratory.

Conclusions

The photochemistry of metallaboranes successfully combines the known organometallic chemistry of the metal fragment with the virtually unknown photochemistry of borane ligands. Irradiation of Fe(η^5-C_5H_5)$(CO)_2$ σ-substituted pentaboranes initiated the dissociation of carbon monoxide, as anticipated based on the chemistry of the [Fe(η^5-C_5H_5)$(CO)_2$R] species. The mass spectral data for compounds **1** and **2** suggested that dissociation of carbon monoxide may be an important reaction of these compounds which may be photochemically induced. Indeed, the largest fragment in the mass spectrum of **1** and **2** was due to the ready loss of carbonyl ligands (see Table 1). The homolytic fission of the iron−cage bond also appears to be a competing pathway in at least the case of the photochemistry of [2,4-(Fe(η^5-C_5H_5)$(CO)_2)_2B_5H_7$] (**2**) complex.

The initial investigations of metallaborane species clearly indicate the potential scope of photochemical processes in cluster chemistry. Importantly, the systems studied appear to provide very high selectivity for single product pathways. This particular feature is anticipated to yield meaningful results and interpretations of the mechanistic studies of accessible cluster photochemical pathways. An understanding of these pathways should provide very valuable insights into the overall chemistry of cluster molecules in general.

Acknowledgment. We thank the National Science Foundation (Grant No. CHE-9521572) and the National Science Foundation Research Experiences for Undergraduates Site Award (Grant No. CHE-8900471), the Donors of the Petroleum Research Fund, administered by the American Chemical Society, the Wright-Patterson Laboratory (Award No. F33615-90-C-5291), and the Industrial Affiliates Program of the Center for Molecular Electronics for support of this work.

Supporting Information Available: A scheme showing the photochemistry of [Fe(η^5-C_5H_5)$(CO)_2$R] complexes, and tables of complete crystallographic data, all atomic coordinates, anisotropic thermal parameters, bond distances and angles involving both non-hydrogen and hydrogen atoms, intermolecular distances for **3** (6 pages); a listing of observed and calculated structure factors (7 pages). The 2D ^{11}B−^{11}B {^{1}H} COSY NMR spectrum of [4-(Fe(η^5-C_5H_5)$(CO)_2$)-2-(η^5-C_5H_5)-2-(CO)-2-FeB_5H_7] (**4**) is available. This material is contained in many libraries on microfiche, immediately follows this article in the microfilm version of the journal, can be ordered from the ACS, and can be downloaded from the Internet; see any current masthead page for ordering information and Internet access instructions.

JA951839V

(44) (a) Fehlner, T. P. *New J. Chem.* **1988**, *12*, 307. (b) Khattar, R.; Puga, J.; Fehlner, T. P.; Rheingold, A. L. *J. Am. Chem. Soc.* **1989**, *111*, 1877. (c) Rath, N. P.; Fehlner, T. P. *J. Am. Chem. Soc.* **1988**, *110*, 5345. (d) Miller, V. R.; Weiss, R.; Grimes, R. N. *J. Am. Chem. Soc.* **1977**, *99*, 5646.